A conditionally cubic-Gaussian stochastic Lagrangian model for acceleration in isotropic turbulence

A. G. LAMORGESE[1]†, S. B. POPE[1], P. K. YEUNG[2] AND B. L. SAWFORD[3]

[1]Sibley School of Mechanical & Aerospace Engineering,
Cornell University, Ithaca, NY 14853-7501, USA

[2]School of Aerospace Engineering, Georgia Institute of Technology,
270 Ferst Drive, Atlanta, GA 30332-0150, USA

[3]Department of Mechanical Engineering, Monash University,
Clayton Campus, Wellington Road, Clayton, VIC 3800, Australia

The modelling of fluid-particle acceleration in homogeneous isotropic turbulence in terms of stochastic models for the Lagrangian velocity, acceleration and a dissipation rate variable is considered. The basis for the Reynolds model (A. M. Reynolds, *Phys. Rev. Lett.* vol. 91, 2003, 084503) is reviewed and examined by reference to direct numerical simulations (DNS) of isotropic turbulence at Taylor-scale Reynolds number (R_λ) up to about 650. In particular, we show DNS data that support stochastic modelling of the logarithm of pseudo-dissipation as an Ornstein–Uhlenbeck process and reveal non-Gaussianity of the acceleration conditioned on fluctuations of the pseudo-dissipation rate. The DNS data are used to construct a new stochastic model that is exactly consistent with Gaussian velocity and conditionally cubic-Gaussian acceleration statistics. This model captures the effects of small-scale intermittency on acceleration and the conditional dependence of acceleration on pseudo-dissipation (which differs from that predicted by the refined Kolmogorov hypotheses). Non-Gaussianity of the conditionally standardized acceleration probability density function (PDF) is accounted for in terms of model nonlinearity. The large-time behaviour of the new model is that of a velocity-dissipation model that can be matched with DNS data for conditional second-order Lagrangian velocity structure functions. As a result, the diffusion coefficient for the new model incorporates two-time information and its Reynolds-number dependence as observed in DNS. The resulting model predictions for conditional and unconditional velocity autocorrelations and time scales are shown to be in very good agreement with DNS.

1. Introduction

The statistics of fluid-particle acceleration in turbulence have been the subject of many experimental (e.g. Voth, Satyanarayan & Bodenschatz 1998; La Porta *et al.* 2001; Christensen & Adrian 2002; Voth *et al.* 2002; Gylfason, Ayyalasomayajula & Warhaft 2004; Mordant *et al.* 2004) and numerical (e.g. Yeung 1997; Vedula & Yeung 1999; Biferale *et al.* 2005; Yeung *et al.* 2006*a*, *b*, 2007) efforts. These investigations

† Present address: CTR/Stanford University, Bldg 500, Stanford, CA 94305, USA.

have spurred a renewed interest in the modelling of conditional and unconditional acceleration statistics in terms of first-order (Beck 2002) and second-order (Pope 2002; Reynolds 2003) Lagrangian stochastic models. Recent work in this area has focused on the construction of stochastic models that are capable of reproducing intermittency and Reynolds-number effects in Lagrangian statistics as observed in experiments and direct numerical simulations (DNS). In other words, second-order stochastic models can be formulated in such a way as to incorporate accurate one-time statistics (and their Reynolds-number dependence) from experiments or DNS and to be able to reproduce intermittent two-time statistics in good agreement with experiments or DNS.

Lagrangian acceleration statistics have been measured in experiments (Voth *et al.* 2002; Mordant *et al.* 2003, 2004) and shown to be (within experimental uncertainties) consistent with the DNS data. In this paper, we assess model performance using a large DNS database on both unconditional (Yeung *et al.* 2006*b*) and conditional (Yeung *et al.* 2007) Lagrangian statistics in isotropic turbulence at Taylor-scale Reynolds numbers up to 650 on a 2048^3 grid.

Reynolds-number effects in Lagrangian stochastic models were first addressed by Sawford (1991). The Sawford (1991) model is exactly consistent with a joint-normal stationary one-time distribution for $Z = [U, A]^T$, where $U(t)$ and $A(t)$ denote (modelled) stochastic processes for one component of the Lagrangian velocity and acceleration. The stochastic differential equations (SDEs) for the Sawford (1991) model are linear:

$$
\mathrm{d}Z = \begin{bmatrix} 0 & 1 \\ -\dfrac{\sigma_A^2}{\sigma_U^2} & -\dfrac{b^2}{2\sigma_A^2} \end{bmatrix} Z \mathrm{d}t + \begin{bmatrix} 0 \\ b \end{bmatrix} \mathrm{d}W, \tag{1.1}
$$

where σ_U and σ_A denote standard deviations for velocity and acceleration, b is a diffusion coefficient, and W is a standard Brownian motion (or Wiener process). Sawford (1991) showed that matching of the second-order Lagrangian velocity structure function $D_U(s) = \langle (U(t+s)-U(t))^2 \rangle$ with the Kolmogorov (1941) hypotheses for the universal equilibrium range uniquely identifies the diffusion coefficient as

$$
b = \sqrt{2\sigma_U^2 \left(T_L^{\infty-1} + t_\eta^{-1} \right) T_L^{\infty-1} t_\eta^{-1}}, \tag{1.2}
$$

where $T_L^\infty = 2\sigma_U^2/(\mathscr{C}_0 \langle \varepsilon \rangle)$ and $t_\eta = \mathscr{C}_0/(2a_0)\sqrt{\nu/\langle \varepsilon \rangle}$. Here, $\mathscr{C}_0$ is the Kolmogorov constant for the second-order Lagrangian velocity structure function, a_0 is the acceleration variance normalized by the Kolmogorov scales, $\langle \varepsilon \rangle$ is the mean dissipation and ν the kinematic viscosity. (Note that t_η is different from the Kolmogorov time scale $\tau_\eta \equiv \sqrt{\nu/\langle \varepsilon \rangle}$.) Sawford (1991) also showed that model predictions are very close to DNS data for unconditional velocity and acceleration autocorrelations at low Reynolds number. However, the Sawford model assumes a Gaussian Lagrangian acceleration PDF and thus does not account for the intermittency of acceleration which has been observed in experiments (La Porta *et al.* 2001) and DNS (Yeung & Pope 1989; Yeung *et al.* 2006*a*).

Reynolds (2003) addressed the problem of incorporating a strongly non-Gaussian PDF of acceleration into a Lagrangian stochastic model. Reynolds showed that an improved representation for the Lagrangian acceleration PDF in a second-order stochastic model can be obtained by explicitly accounting for intermittency of dissipation. Specifically, he assumed a log-normal distribution for the dissipation rate, ε, together with a Gaussian assumption for the conditional PDF of $A|\varepsilon$. The

latter assumption can be restated in terms of the *conditionally standardized acceleration* defined by $\tilde{A} \equiv A/\sigma_{A|\varepsilon}$ (which has zero and unit values for its conditional mean and variance) where $\sigma_{A|\varepsilon}^2$ is the conditional acceleration variance. In the Reynolds model, the conditional distribution $\tilde{A}|\varepsilon$ is assumed to be universal and, in particular, standard normal. This can be interpreted to imply that intermittency of dissipation is solely responsible for intermittency in acceleration. Reynolds also assumed, at the one-time level, Gaussian velocity statistics and independence of velocity from dissipation and acceleration. In other words, the Reynolds model is (by construction) exactly consistent with a joint-normal stationary one-time distribution of $(U, \tilde{A}, \ln \varepsilon)$.

To completely specify his model, Reynolds extended the Kolmogorov (1962) reasoning to obtain the following prediction for the conditional acceleration variance,

$$\sigma_{A|\varepsilon}^2 / a_\eta^2 = a_0^* (\varepsilon/\langle \varepsilon \rangle)^{3/2}, \tag{1.3}$$

where a_0^* is a constant (taken to be 3.3) and $a_\eta = (\langle \varepsilon \rangle^3/\nu)^{1/4}$ is the Kolmogorov acceleration scale. Following Pope & Chen (1990), Reynolds also assumed an Ornstein–Uhlenbeck process for $\chi \equiv \ln \varepsilon$. The resulting model can be written as an SDE for $\mathbf{Z}$ redefined as $\mathbf{Z} = [U, \tilde{A}, \ln \varepsilon - \langle \ln \varepsilon \rangle]^T$:

$$\mathrm{d}\mathbf{Z} = \begin{bmatrix} 0 & \sigma_{A|\varepsilon} & 0 \\ -\dfrac{\sigma_{A|\varepsilon}}{\sigma_U^2} & -\dfrac{b^2}{2\sigma_{A|\varepsilon}^2} & 0 \\ 0 & 0 & -T_\chi^{-1} \end{bmatrix} \mathbf{Z} \, \mathrm{d}t + \begin{bmatrix} 0 & 0 \\ b/\sigma_{A|\varepsilon} & 0 \\ 0 & \sqrt{2\sigma_\chi^2/T_\chi} \end{bmatrix} \begin{bmatrix} \mathrm{d}W \\ \mathrm{d}W' \end{bmatrix}. \tag{1.4}$$

In these equations, σ_χ and T_χ denote the standard deviation and the integral scale for χ, whereas W and W' are independent Wiener processes. The dissipation equation is effectively decoupled from the rest of the system and therefore the Reynolds model is linear in U and $\tilde{A}$. Note, however, that $\sigma_{A|\varepsilon}$ depends on $\chi(t)$. Additional assumptions made by Reynolds are: (i) a choice of diffusion coefficient made by analogy with the Sawford (1991) model, i.e.

$$b = \sqrt{2\sigma_U^2 (T_{L,\varepsilon}^{-1} + t_{\eta,\varepsilon}^{-1}) T_{L,\varepsilon}^{-1} t_{\eta,\varepsilon}^{-1}}, \tag{1.5}$$

where $T_{L,\varepsilon} = 2\sigma_U^2/(C_0 \varepsilon)$ and $t_{\eta,\varepsilon} = C_0/(2a_0^*)\sqrt{\nu/\varepsilon}$ (C_0 being a model constant, taken equal to 7), and (ii) $T_\chi \langle \varepsilon \rangle / \sigma_U^2 = 2/C_0$.

In this paper, we first review the basis for the Reynolds model against DNS. Then, a novel stochastic model is constructed for the Lagrangian velocity, acceleration and pseudo-dissipation (referred to as the U–A–χ model) that incorporates one-time information from DNS and yields model predictions for two-time velocity statistics in good agreeement with DNS. In §2, we review DNS data (first presented in Yeung *et al.* 2006a) for intermittency of dissipation, the PDF of conditionally standardized acceleration and the variance of acceleration conditioned on the pseudo-dissipation. In §3, a novel stochastic U–A–χ model that incorporates non-Gaussian one-time statistics from DNS is formulated. Non-Gaussianity of the conditionally standardized acceleration PDF is accounted for in terms of nonlinearity in the model. At high Reynolds number and for times much larger than τ_η, the statistics of the U–A–χ model are given more simply by a U–χ (or velocity-dissipation) model. The U–χ model can be deduced from the U–A–χ model by a systematic procedure known as adiabatic elimination, which is described in, e.g. Gardiner (2004, §6.4 therein) and described further in the present context in §4 and Appendix A. For example, adiabatic elimination of acceleration from the Sawford (1991) model yields a Langevin

model for velocity with integral time scale T_L^∞. In §5, we show a choice of diffusion coefficient for the U–A–χ model that is based on the adiabatic elimination result and the observation that the U–χ model can be matched with DNS data for conditional two-time velocity statistics. In §6, the resulting model predictions for conditional and unconditional velocity autocorrelations and time scales are shown to be in good agreement with DNS. Conclusions for this work are summarized in §7. Appendix A shows a detailed derivation of the U–χ model, and some of its properties are deduced in Appendix B.

2. DNS data for stochastic modelling

2.1. *Intermittency of dissipation*

The Lagrangian stochastic model developed in this paper draws heavily upon an Eulerian study of acceleration and dissipation intermittency using DNS (Yeung *et al.* 2006*a*). For the sake of self-completeness, in this paper we summarize here selected aspects of the DNS results of greatest relevance to our modelling approach. The simulations are performed on grids up to 2048^3, on the largest of which the Taylor-scale Reynolds number is $R_\lambda \approx 650$, where R_λ is defined as $R_\lambda \equiv \sigma_U \lambda / \nu$ with λ calculated according to the local isotropy relation $\lambda = \sqrt{15\nu\sigma_U^2/\langle\varepsilon\rangle}$. The dissipation-like variables considered are ε, ζ and φ, where $\varepsilon = 2\nu s_{ij}s_{ij}$ is the dissipation rate, $\zeta = 2\nu r_{ij}r_{ij}$ is the 'enstrophy' (s_{ij} and r_{ij} being the strain-rate and rotation-rate tensors) and $\varphi = (\varepsilon + \zeta)/2$ is the pseudo-dissipation.

Figure 4 of Yeung *et al.* (2006*a*) shows the standardized PDFs of $\ln\varepsilon$, $\ln\zeta$ and $\ln\varphi$ from the DNS at $R_\lambda \approx 650$ in comparison to the standard Gaussian (corresponding to a log-normal distribution for the dissipation variables). As can be seen from that figure, especially from the left-hand tail, pseudo-dissipation (as opposed to the dissipation rate, or the enstrophy) is closest to log-normal for $R_\lambda \approx 650$. In fact, DNS data support this conclusion for Reynolds numbers in the range $R_\lambda \approx 140 - 650$. In this paper, we do not purport to discuss the validity of the log-normal model as opposed to more accurate intermittency models for dissipation (see, e.g. Frisch 1995). We limit ourselves to the observation that pseudo-dissipation can be described approximately as log-normal for $R_\lambda \approx 140 - 650$. It should be noted that, although their PDFs and other statistics differ, ε, ζ and φ have the same mean values in homogeneous turbulence.

We now investigate the hypothesis that χ redefined in terms of φ (i.e. $\chi(t) = \ln\varphi(t)/\langle\varepsilon\rangle$) can be modelled by an Ornstein–Uhlenbeck process, as proposed by Pope & Chen (1990):

$$\mathrm{d}\chi = -\left(\chi + \frac{\sigma_\chi^2}{2}\right)\frac{\mathrm{d}t}{T_\chi} + \sqrt{\frac{2\sigma_\chi^2}{T_\chi}}\,\mathrm{d}W'. \qquad (2.1)$$

This model predicts the two-time conditional mean $\langle X(s)|X(0) = x\rangle = x\exp(-s/T_\chi)$ for $s \geqslant 0$, where X is the standardized logarithm of pseudo-dissipation $X \equiv (\ln\varphi - \langle\ln\varphi\rangle)/\sigma_{\ln\varphi}$ (with $\sigma_{\ln\varphi}$ denoting the root mean square (r.m.s.) value of $\ln\varphi$). It follows that the autocorrelation function of $X(t)$ is exponential with time scale T_χ. Figure 1 shows (Lagrangian) two-time conditional means of X from DNS compared to the exponentials corresponding to the Ornstein–Uhlenbeck process. Figure 2 shows two-time conditional means from DNS with X redefined in terms of ε. As can be seen from figure 1, the two-time conditional means of the (standardized) logarithm of pseudo-dissipation are close to exponentials. The same conclusion is supported by
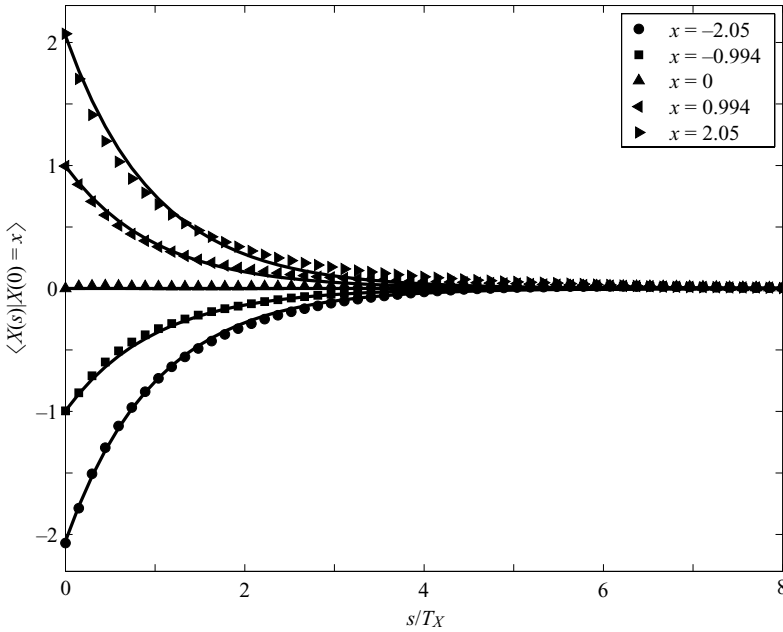
FIGURE 1. Data from 1024^3 DNS (with $R_\lambda \approx 390$) for conditional expectations (symbols) with $X = (\ln \varphi - \langle \ln \varphi \rangle)/\sigma_{\ln \varphi}$ compared to $x \exp(-s/T_X)$ (solid, with T_X denoting the Lagrangian integral time scale for X).
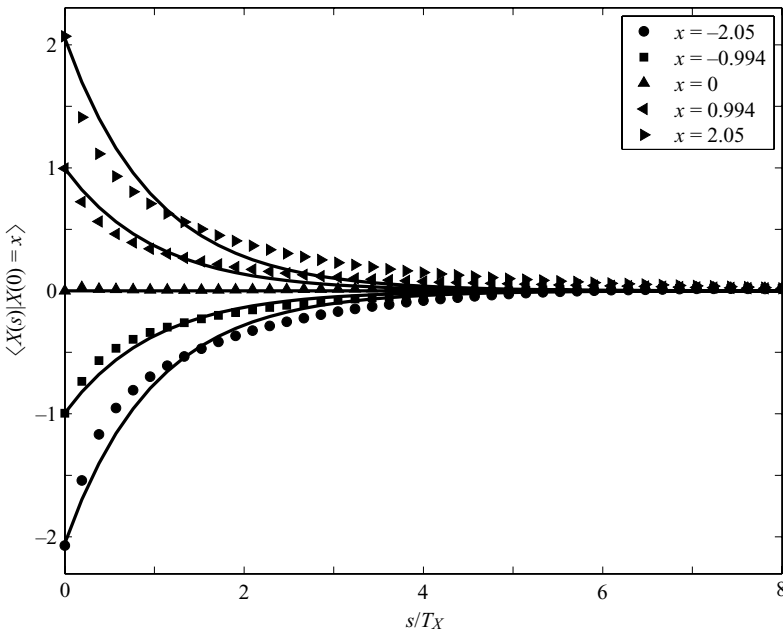

FIGURE 2. As figure 1, but $X = (\ln \varepsilon - \langle \ln \varepsilon \rangle)/\sigma_{\ln \varepsilon}$.

the DNS over the range of R_λ studied. In contrast, it can be seen from figure 2 that the two-time conditional means of the (standardized) logarithm of dissipation rate deviate significantly from exponential. Therefore, on the basis of DNS, we argue that,
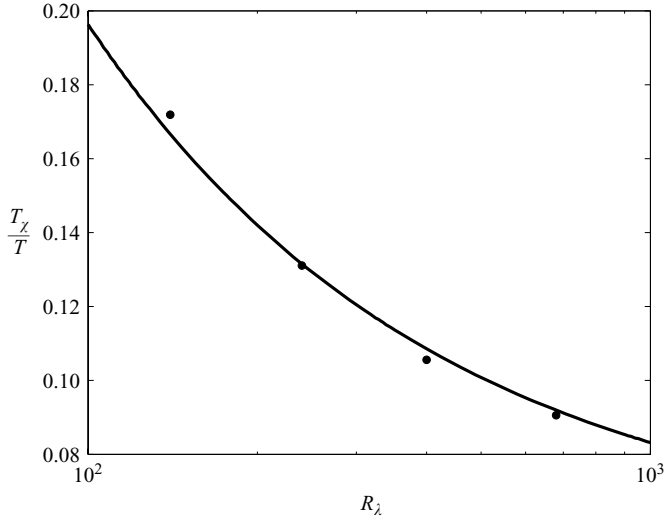
FIGURE 3. Integral time scale of $\chi(t)$, T_χ, normalized by $T \equiv (3/2)\sigma_U^2/\langle\varepsilon\rangle$, as a function of Reynolds number: symbols, DNS data; line, the empirical relation, (2.3).

for the purposes of stochastic modelling, pseudo-dissipation is well-approximated by an Ornstein–Uhlenbeck process.

To completely specify the dissipation model (2.1), σ_χ and T_χ have to be prescribed. As discussed by Yeung *et al.* (2006*a*), the DNS data support the Kolmogorov (1962) prediction for

$$\sigma_\chi^2 = A + \frac{3\mu}{2}\ln R_\lambda, \qquad (2.2)$$

with $\mu = 0.25$, in good agreement with Sreenivasan & Kailasnath (1993) ($A = -0.863$ is reported by Yeung *et al.* 2006*a*).

Figure 3 shows DNS data for the integral time scale T_χ normalized by $T \equiv (3/2)\sigma_U^2/\langle\varepsilon\rangle$. As can be seen, over the range of R_λ investigated, this is represented well by the empirical relation

$$\frac{T_\chi}{T} = 0.055 + \frac{3.55}{R_\lambda^{0.7}}, \qquad (2.3)$$

and this is the specification used in the model. This relation has no theoretical basis, but yields the plausible asymptote of T_χ/T tending to a positive constant as R_λ tends to infinity. Reynolds-number dependences in the two-time statistics of the pseudo-dissipation are examined in more detail in a companion paper (Yeung *et al.* 2007).

2.2. *PDF of conditionally standardized acceleration*

Recall that $\tilde{A}(t) = A(t)/\sigma_{A|\varepsilon}(\varepsilon(t))$ is the conditionally standardized acceleration, i.e. the acceleration $A(t)$ normalized by the standard deviation of acceleration conditional on the current value of dissipation, $\sigma_{A|\varepsilon}(\varepsilon(t))$. The PDF of $\tilde{A}(t)$ conditional on $\varepsilon(t) = \hat{\varepsilon}$ is denoted by $f_{\tilde{A}|\varepsilon}(\tilde{a}|\hat{\varepsilon})$, where $\tilde{a}$ is a sample space variable corresponding to $\tilde{A}$. In the Reynolds model, it is assumed that $f_{\tilde{A}|\varepsilon}(\tilde{a}|\hat{\varepsilon})$ is a standard Gaussian (independent of $\hat{\varepsilon}$). Figure 14 of Yeung *et al.* (2006*a*) shows conditional PDFs $f_{\tilde{A}|\varepsilon}(\tilde{a}|\hat{\varepsilon})$ for different values of the dissipation $\hat{\varepsilon}$ for $R_\lambda \approx 650$. Figure 15 of Yeung *et al.* (2006*a*) shows analogous information when the pseudo-dissipation φ is used as the conditioning variable in

place of ε (that is, $\tilde{A}$ is redefined as $\tilde{A} = A/\sigma_{A|\varphi}$, where $\sigma_{A|\varphi}$ is the standard deviation of acceleration conditioned on the pseudo-dissipation). Both sets of conditional PDFs show much less intermittency (with weaker tails at large fluctuations) than the unconditional acceleration PDF. This is particularly true of the PDFs of $\tilde{A}|\varphi$ (with $\tilde{A} = A/\sigma_{A|\varphi}$) which, however, still show significant non-Gaussian behaviour. A remarkable degree of collapse of these PDFs for different values of the conditioning variable is notable (except for very small and very large conditional fluctuations). Therefore, to a first approximation, the PDFs $f_{\tilde{A}|\hat{\varphi}}$ can be described as approximately independent of $\hat{\varphi}$. In fact, based on simulations at different Reynolds numbers (Yeung *et al.* 2006*a*), the conditional PDF of $\tilde{A}|\varphi$ can also be (approximately) described as independent of the Reynolds number.

Yeung *et al.* (2006*a*) suggest that the PDF of $\tilde{A}|\varphi$ can be described (to a very good approximation) as cubic-Gaussian. By definition, a standardized random variable V is cubic-Gaussian with parameter p (also denoted as $V \sim G^3(p)$) if

$$V = C[(1 - p)g + pg^3], \tag{2.4}$$

where g is a standardized Gaussian random variable and C is determined by the standardization condition $\langle V^2 \rangle = 1$ as $C(p) = (1 + 4p + 10p^2)^{-1/2}$. Figure 16 of Yeung *et al.* (2006*a*) compares the conditional acceleration PDFs obtained from DNS (at $R_\lambda \approx 650$) to the cubic-Gaussian on both linear and logarithmic scales. As can be seen, the cubic-Gaussian PDF provides a remarkably accurate description of the conditional PDF $f_{\tilde{A}|\varphi}$. Comparable accuracy is achieved when the cubic-Gaussian PDF is used to represent DNS data for $f_{\tilde{A}|\varphi}$ at lower Reynolds numbers (not shown, but see §IV of Yeung *et al.* 2006*a*). A value of $p \approx 0.1$ results from the observation (based on DNS) that the kurtosis of the conditional acceleration is approximated well as $\mu_4(\tilde{A}|\hat{\varphi}) \approx 8$ (approximately independent of $\hat{\varphi}$ and R_λ; more details are provided by Yeung *et al.* 2006*a*).

2.3. *Conditional acceleration variance*

With a view to the joint (stochastic) modelling of acceleration and pseudo-dissipation, we now investigate the validity of the Reynolds (2003) prediction for the conditional acceleration variance,

$$\sigma_{A|\varphi}^2 / a_\eta^2 = a_0^*(\varphi/\langle\varepsilon\rangle)^{3/2}, \tag{2.5}$$

which follows from an extension of the Kolmogorov (1962) hypotheses. Figure 11 of Yeung *et al.* (2006*a*) shows φ-dependences from DNS for the conditional acceleration variance at different Reynolds numbers. In the same figure, the following expression (first presented in Yeung *et al.* 2006*a*)

$$\frac{\sigma_{A|\varphi}^2}{a_\eta^2} = \frac{1.2}{R_\lambda^{0.2}} \left(\frac{\varphi}{\langle\varepsilon\rangle}\right)^{0.15} + \ln\left(\frac{R_\lambda}{20}\right)\left(\frac{\varphi}{\langle\varepsilon\rangle}\right)^{1.25}, \tag{2.6}$$

is shown to be an accurate representation (except at the smallest R_λ) of the DNS data. As can be seen, the low-φ behaviour for the conditional acceleration variance deviates strongly from that predicted by (2.5). Also, careful measurement of the slope for the large-φ portion of the curves yields values that are systematically less than 1.5, again at variance with the Kolmogorov (1962) prediction.

Equation (2.6) is most useful for stochastic modelling purposes because it accurately parameterizes the conditional acceleration variance (given φ) in terms of both the conditioning variable and the Reynolds number.

3. Conditionally cubic-Gaussian (CCG) stochastic Lagrangian models

As outlined in the previous section, Lagrangian statistics for ε, ζ and φ from DNS (Yeung *et al.* 2007) show that an accurate stochastic model for acceleration is most easily developed when pseudo-dissipation is used in place of the dissipation rate or the enstrophy as a component of the model. This is because (i) φ is closest to log-normal, (ii) two-time conditional means of $\ln \varphi$ are closest to exponential, and (iii) the conditional PDFs of acceleration given $\varphi = \hat{\varphi}$ collapse best, and with the least degree of non-Gaussianity. Thus, we base the model on pseudo-dissipation φ and take the Ornstein–Uhlenbeck process, (2.1), as its stochastic model.

Conditioning on pseudo-dissipation is most useful when considering the joint-statistics of acceleration and pseudo-dissipation because the PDF of $\tilde{A}|\varphi$ can be described (to a first approximation) as universal and, in particular, cubic-Gaussian. In other words, given $\varphi = \hat{\varphi}$ and a standardized Gaussian random variable $\bar{A}$, the acceleration A can be modelled as

$$A = \sigma_{A|\hat{\varphi}} C[(1-p)\bar{A} + p\bar{A}^3]. \tag{3.1}$$

The stochastic model is most conveniently expressed in terms of the velocity $U(t)$, the Gaussian 'acceleration' $\bar{A}(t)$ (related to the acceleration by (3.1)), and the variable $\chi^* \equiv \chi - \langle \chi \rangle = \ln \varphi - \langle \ln \varphi \rangle$, which is the logarithm of the pseudo-dissipation with its mean removed. Note that the process $\bar{A}(t)$ is non-dimensional, and it is constructed to have zero mean, unit variance and a Gaussian one-time PDF.

The conditionally cubic-Gaussian (CCG) model introduced here is defined by the stochastic differential equations

$$dU = A\,dt = \sigma_{A|\varphi} C[(1-p)\bar{A} + p\bar{A}^3]\,dt, \tag{3.2}$$

$$d\bar{A} = \bar{\theta}\,dt + \bar{b}\,dW, \tag{3.3}$$

$$d\chi^* = -\chi^* \frac{dt}{T_\chi} + \sqrt{\frac{2\sigma_\chi^2}{T_\chi}}\,dW', \tag{3.4}$$

where $\bar{\theta}$ and $\bar{b}$ are drift and diffusion coefficients specified below. All of the other coefficients are as specified above, namely, $p = 0.1$, $C = (1 + 4p + 10p^2)^{-1/2} = \sqrt{2/3}$, $\sigma_{A|\varphi}^2$ is given by (2.6), σ_χ^2 is given by (2.2), and T_χ is given by (2.3).

The stationary one-time joint PDF of U, $\bar{A}$ and χ^* is denoted by $f(v, \bar{a}, x^*)$, where $v, \bar{a}$ and x^* are sample-space variables corresponding to U, $\bar{A}$ and χ^*. This joint PDF is governed by the Fokker–Planck equation which can be derived from (3.2)–(3.4). A constraint imposed on the model is that this PDF is joint-normal with the variables uncorrelated with each other, i.e.

$$f = \frac{1}{\sigma_U \sqrt{2\pi}} \exp\left(-\frac{v^2}{2\sigma_U^2}\right) \frac{1}{\sqrt{2\pi}} \exp\left(-\frac{\bar{a}^2}{2}\right) \frac{1}{\sigma_\chi \sqrt{2\pi}} \exp\left(-\frac{x^{*2}}{2\sigma_\chi^2}\right). \tag{3.5}$$

The imposition of this PDF in the Fokker–Planck equation for $f(v, \bar{a}, x^*)$ leads to a constraint for the drift coefficient $\bar{\theta}$ in (3.3), namely,

$$\bar{\theta}(v, \bar{a}, \varphi) = -\frac{\sigma_{A|\varphi}}{\sigma_U^2} Cv(1 + p + p\bar{a}^2) + \frac{\bar{b}^2}{2} \frac{\partial}{\partial \bar{a}} \ln \bar{b}^2 f. \tag{3.6}$$

We take the diffusion coefficient $\bar{b}$ to be a function of φ. Then, (3.3) can be rewritten as

$$\mathrm{d}\bar{A} = -\frac{\bar{b}^2}{2}\bar{A}\,\mathrm{d}t - \frac{\sigma_{A|\varphi}}{\sigma_U^2}UC(1+p+p\bar{A}^2)\,\mathrm{d}t + \bar{b}\,\mathrm{d}W. \tag{3.7}$$

This equation (together with (3.2) and (3.4)) defines a class of CCG models, i.e. different models with the same stationary distribution (3.5) correspond to different choices of $\bar{b}$. Each model captures the conditional dependence of acceleration on pseudo-dissipation based on DNS (equation (2.6)) that accounts for deviations from the Kolmogorov (1962) hypotheses. Also, each model is nonlinear because it accounts for the non-Gaussianity of the conditionally standardized acceleration PDF.

The specification of the diffusion coefficient is presented in §5. This is based in part on properties of the corresponding velocity–dissipation model which we discuss next in §4.

4. Corresponding velocity–dissipation model

At high Reynolds number, there is a separation between the characteristic time scale of the acceleration (proportional to the Kolmogorov time scale τ_η) and the characteristic time scale of the velocity correlations (proportional to T). Consequently, for intermediate time intervals δt ($\tau_\eta \ll \delta t \ll T$), the velocity increment $\Delta_{\delta t}U(t) \equiv U(t+\delta t) - U(t)$ given by the CCG model (equation (3.2)) is approximated well by a Gaussian random variable whose mean and variance are both proportional to δt and depend on $U(t)$ and $\chi(t)$, but not on $A(t)$. That is, there are coefficients $\mu(v, \hat{\chi})$ and $\Sigma(v, \hat{\chi})$ such that, asymptotically as both $\tau_\eta/\delta t$ and $\delta t/T$ tend to zero,

$$\langle \Delta_{\delta t}U(t)|U(t) = v, A(t) = a, \chi(t) = \hat{\chi}\rangle/\delta t \to \mu(v, \hat{\chi}), \tag{4.1}$$

$$\langle (\Delta_{\delta t}U(t))^2|U(t) = v, A(t) = a, \chi(t) = \hat{\chi}\rangle/\delta t \to \Sigma(v, \hat{\chi}). \tag{4.2}$$

It then follows that (in the limit considered) $U(t)$ and $\chi(t)$ evolve by the $U-\chi$ model

$$\mathrm{d}U = \mu(U, \chi)\,\mathrm{d}t + \sqrt{\Sigma(U, \chi)}\,\mathrm{d}W, \tag{4.3}$$

$$\mathrm{d}\chi = -\left(\chi + \frac{\sigma_\chi^2}{2}\right)\frac{\mathrm{d}t}{T_\chi} + \sqrt{\frac{2\sigma_\chi^2}{T_\chi}}\,\mathrm{d}W'. \tag{4.4}$$

This form of model was proposed by Pope & Chen (1990) with the specification

$$\Sigma = \mathscr{C}_0\langle\varepsilon\rangle\mathrm{e}^\chi. \tag{4.5}$$

At moderate and high Reynolds numbers, the $U-\chi$ model provides an approximation to the $U-A-\chi$ model in the following sense: for one-time statistics, and for multi-time statistics defined by time intervals which are large compared to the Kolmogorov time scale, the statistics of $U(t)$ and $\chi(t)$ generated by the $U-\chi$ model approximate those generated by the $U-A-\chi$ model.

The procedure of adiabatic elimination (Theiss & Titulaer 1985; Gardiner 2004) has previously been applied to a stochastic model for velocity and acceleration by Pope (2002). Also, when applied to Sawford's model, it yields the Langevin equation with integral time scale T_L^∞. However, for technical reasons, the application of adiabatic elimination to the CCG $U-A-\chi$ model is involved and the details are relegated to Appendix A. Briefly, the method of multiple scales is applied to the Fokker–Planck equation corresponding to the CCG model. This identifies the coefficients $\mu(v, \hat{\chi})$ and
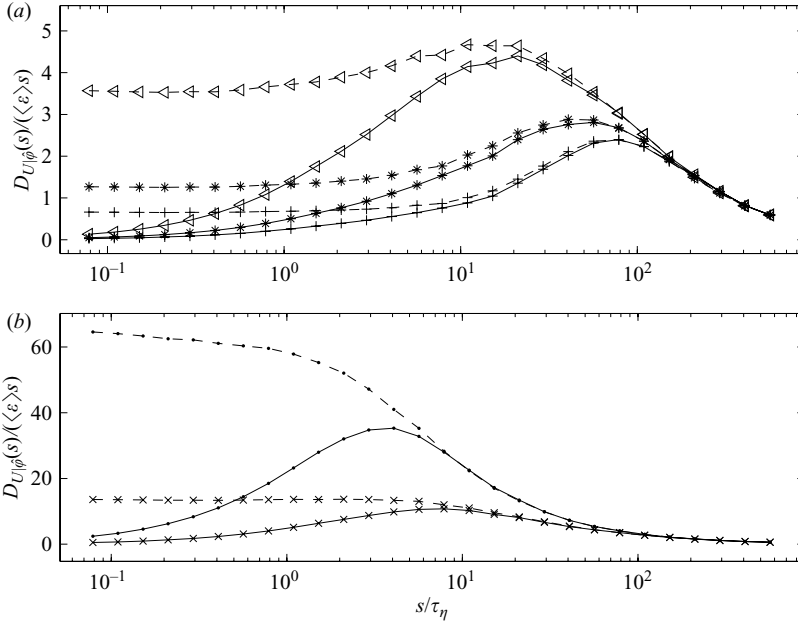
FIGURE 4. Conditional second-order Lagrangian velocity structure functions for the CCG model (solid) with $\bar{b} = \mathrm{const}$ compared to velocity–dissipation model (4.6)–(4.7) with $\mathscr{T}_{L,\varphi}$ obtained from (4.8) (dashed). The symbols {+, ∗, triangle, ×, small circle} correspond to the values (a) {−2.05, −0.994, 0} and (b) {0.994, 2.05} of the conditioning variable $(\ln\varphi - \langle\ln\varphi\rangle)/\sigma_{\ln\varphi}$.

$\Sigma(v, \hat{\chi})$ so that the corresponding U–χ model can be written

$$\mathrm{d}U = -\frac{U}{\mathscr{T}_{L,\varphi}}\,\mathrm{d}t + \sqrt{\frac{2\sigma_U^2}{\mathscr{T}_{L,\varphi}}}\,\mathrm{d}W, \tag{4.6}$$

$$\mathrm{d}\chi = -\left(\chi + \frac{\sigma_\chi^2}{2}\right)\frac{\mathrm{d}t}{T_\chi} + \sqrt{\frac{2\sigma_\chi^2}{T_\chi}}\,\mathrm{d}W', \tag{4.7}$$

where

$$\frac{\mathscr{T}_{L,\varphi}}{T} \approx \frac{\tau_\eta \bar{b}^2}{3\delta(\sigma_{A|\varphi}/a_\eta)^2}, \tag{4.8}$$

with $\delta \equiv C^2(1 + 4p + 6p^2) \approx 0.97$ and $T \equiv 1.5\sigma_U^2/\langle\varepsilon\rangle$. These relations are obtained in Appendix A from a multiple-scales treatment of the Fokker–Planck equation associated with (3.7), (3.2) and (3.4). The validity of (4.8) is tested numerically in figure 4, where second-order conditional Lagrangian velocity structure functions for the CCG (with $\bar{b} = 11.7\,s^{-1/2}$) are compared to those obtained using the velocity–dissipation model, (4.6), (4.7), with $\mathscr{T}_{L,\varphi}$ obtained from (4.8). For each value of the conditioning variable, at large time lags s, there is excellent agreement between structure functions according to the two models. As s decreases, at some point the two predictions deviate from each other: for $s/\tau_\eta \ll 1$, that given by the CCG model correctly varies as $D_{U|\varphi}(s) \sim s^2$ (corresponding to $A(t)$ being continuous); whereas that given by the U–χ model varies linearly with s (corresponding to $A(t)$ being

modelled as white noise). For $s/\tau_\eta \geqslant 30$, the difference between the two models is less than 5 %.

In Appendix B, we show that the conditional Lagrangian velocity structure functions implied by the velocity–dissipation model at each value of the time lag are given as a nonlinear functional of an Ornstein–Uhlenbeck process. The consequences of this and (4.8) are investigated in the next section.

5. Specification of the diffusion coefficient

The CCG model has been constructed to yield the observed one-time statistics of velocity, acceleration and pseudo-dissipation, and the observed conditional autocorrelations of pseudo-dissipation. It remains to specify the diffusion coefficient $\bar{b}$ (as a function of φ and R_λ) which determines the two-time statistics of velocity and acceleration. It is simplest to state the specification used, present some results, and then explain how the specification was developed.

Drawing on (4.8), we specify the diffusion coefficient via $\mathscr{T}_{L,\varphi}$ as

$$\bar{b}^2 = \frac{3\delta(\sigma_{A|\varphi}/a_\eta)^2}{\tau_\eta} \frac{\mathscr{T}_{L,\varphi}}{T}, \tag{5.1}$$

with the specifications

$$\frac{T}{\mathscr{T}_{L,\varphi}} = \alpha + \beta \left(\frac{\varphi}{\langle \varepsilon \rangle}\right)^{1/2}, \tag{5.2}$$

$$\alpha = 2.9, \quad \beta = \beta_0 \sqrt{R_\lambda}, \quad \beta_0 = 0.16. \tag{5.3}$$

The most revealing two-time velocity statistic is the conditional second-order velocity structure function

$$D_{U|\varphi}(s|\hat{\varphi}) = \langle [U(s) - U(0)]^2 | \varphi(0) = \hat{\varphi} \rangle. \tag{5.4}$$

Figure 5 shows this quantity, normalized by $\langle \varepsilon \rangle s$, obtained from the DNS data, from the CCG model, and from the corresponding velocity–dissipation model, at $R_\lambda \approx 650$. The diffusion coefficient $\bar{b}$ is specified to match, to the extent possible, the values of $D_{U|\varphi}$ from the CCG model with those from the DNS. These values match well for times $s/\tau_\eta \geqslant 20$. For the smallest conditioning values of pseudo-dissipation, this matching extends to all times. However, for large values of the conditioning variable, there are significant discrepancies at intermediate times (e.g. $1 < s/\tau_\eta < 10$). Our experience strongly suggests that there is no specification of $\bar{b}$ which results in accurate predictions of $D_{U|\varphi}(s|\hat{\varphi})$ for all s and $\hat{\varphi}$. Hence the focus is on achieving the best matching possible, especially at large times (e.g. $s/\tau_\eta \geqslant 20$).

Also shown in figure 5 are the values of $D_{U|\varphi}$ obtained from the velocity–dissipation model. These agree well with the CCG model and the DNS for large times ($s/\tau_\eta \geqslant 20$), but are qualitatively different at small times. Specifically, the velocity–dissipation model predicts

$$\lim_{s \to 0} \frac{D_{U|\varphi}(s|\hat{\varphi})}{\langle \varepsilon \rangle s} = \frac{4T}{3\mathscr{T}_{L,\varphi}(\hat{\varphi})}. \tag{5.5}$$

In the CCG model, for $s/T_\chi \ll 1$, $\varphi(s)$ is little different from $\varphi(0)$, and so $D_{U|\varphi}(s|\hat{\varphi})$ is dominantly affected by $\mathscr{T}_{L,\varphi}(\hat{\varphi})$ (for the same value of $\hat{\varphi}$). Hence, increasing $T/\mathscr{T}_{L,\varphi}(\hat{\varphi})$ tends to increase the value of $D_{U|\varphi}(s|\hat{\varphi})$ given by the CCG model (for the same value of $\hat{\varphi}$). This observation is the basis for an iterative trial-and-error method to determine the specification of $T/\mathscr{T}_{L,\varphi}$ which matches $D_{U|\varphi}(s|\hat{\varphi})$ given by the CCG
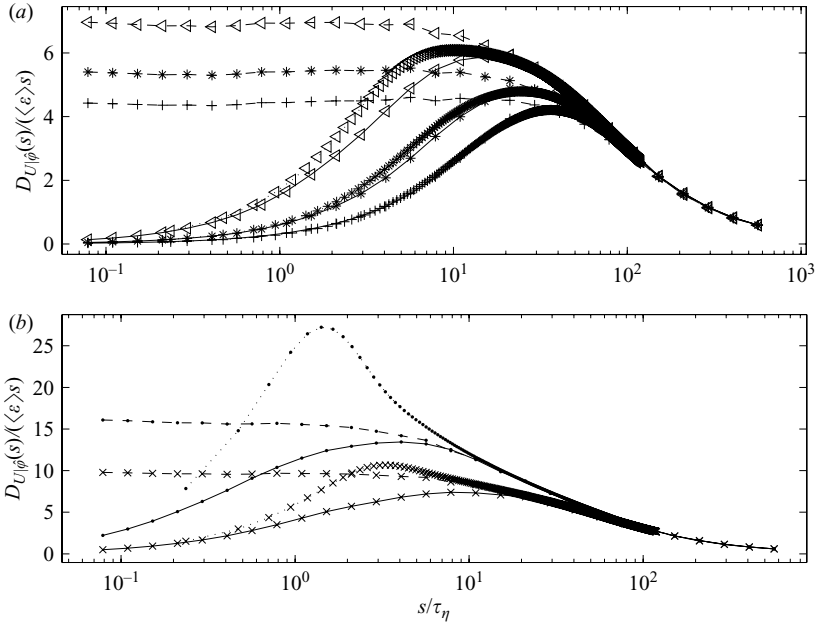
FIGURE 5. Conditional second-order Lagrangian velocity structure functions for the CCG (solid) based on (5.2)–(5.3) and velocity–dissipation (dashed) models compared to data at $R_\lambda \approx 650$ from 2048^3 DNS (dotted). The symbols are as in figure 4.

model to the DNS data for $s/\tau_\eta \geqslant 20$. We carried out the trial-and-error procedure using DNS data at four different Reynolds numbers and observed that the variation of $T/\mathcal{T}_{L,\varphi}$ thus deduced can be reasonably approximated by (5.2)–(5.3).

It is interesting to observe the form of the time scale $\mathcal{T}_{L,\varphi}$ implied by the specifications (5.1)–(5.2) at small and large values of the pseudo-dissipation. For $\varphi/\langle\varepsilon\rangle \ll 1$, (5.2) yields

$$\mathcal{T}_{L,\varphi} \approx T/\alpha, \tag{5.6}$$

i.e. $\mathcal{T}_{L,\varphi}$ is proportional to the large-scale time scale, independent of φ. In contrast, for $\varphi/\langle\varepsilon\rangle \gg 1$, (5.2) yields

$$\mathcal{T}_{L,\varphi} \approx \frac{T}{\beta_0 R_\lambda^{1/2}(\varphi/\langle\varepsilon\rangle)^{1/2}}$$

$$= \frac{\sqrt{T\tau_\eta}}{\beta_0(20/3)^{1/4}}\sqrt{\frac{\langle\varepsilon\rangle}{\varphi}}. \tag{5.7}$$

Thus, as $\varphi/\langle\varepsilon\rangle$ increases from small to large values, $\mathcal{T}_{L,\varphi}$ decreases from a mean large-scale time scale to a local micro-scale time scale (that is, much less than $\sqrt{T\tau_\eta}$ for $\varphi/\langle\varepsilon\rangle \gg 1$).

It should be noted that the velocity–dissipation model obtained after adiabatic elimination of acceleration from the Reynolds (2003) model has a diffusion coefficient Σ that is formally identical to the Pope & Chen (1990) model, (4.5). In contrast, the χ-dependence of Σ after adiabatic elimination of acceleration from the CCG model is given by (5.2).
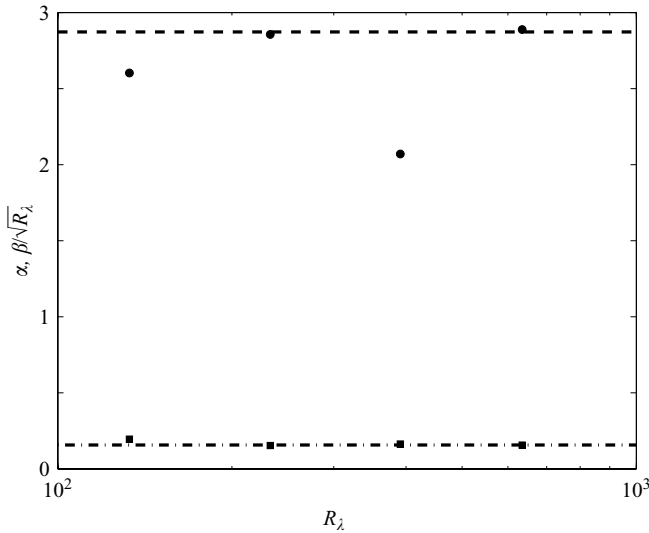
FIGURE 6. Values of α (circles) and $\beta/\sqrt{R_\lambda}$ (squares) in (5.2) deduced from DNS data compared to (5.3) (dashed and dot-dashed).

6. Comparison of stochastic models with DNS data

In this section, we examine the performance of different stochastic models based on comparisons with DNS data, which include unconditional statistics (Yeung *et al.* 2006 *b*) and conditional statistics (Yeung *et al.* 2007). Some of the DNS data for comparison (e.g. conditional velocity autocorrelations) are taken directly from Yeung *et al.* (2007) whereas others (e.g. conditional velocity structure function) have been computed explicitly from the same DNS database which covers R_λ from 40 to 650 on 64^3 to 2048^3 grids.

The models considered are: the CCG model; the corresponding velocity–dissipation model; the Reynolds (2003) model; and Sawford's (1991) model. For the CCG model, results are reported for the coefficients α and β in (5.2) obtained both from the DNS data (see figure 6) and from the specification (5.3). For the highest Reynolds number ($R_\lambda \approx 650$), we first present unconditional and then conditional statistics; and then the Reynolds-number dependence of key quantities is considered.

6.1. *Unconditional statistics*

Figure 7 compares the Lagrangian velocity autocorrelation functions given by the different models with the DNS data. As with all statistics at $R_\lambda \approx 650$, there is little difference between the CCG predictions based on the two slightly different specifications of the coefficients, and these agree well with the DNS data. The velocity autocorrelation function given by the CCG model is very close to exponential. In contrast, the Reynolds model significantly overestimates the autocorrelation time scale. Improved agreement with DNS for the Reynolds model should be possible by further 'tuning' of the parameters a_0^* and C_0.

The acceleration autocorrelations are shown in figure 8. It is clear that stochastic models of the type considered are not capable of representing the short-time ($s/\tau_\eta < 1$) behaviour accurately. The autocorrelation function from the DNS is parabolic for small times with zero slope at the origin, reflecting the fact that the Lagrangian acceleration given by the Navier–Stokes equations is differentiable in time. In contrast,
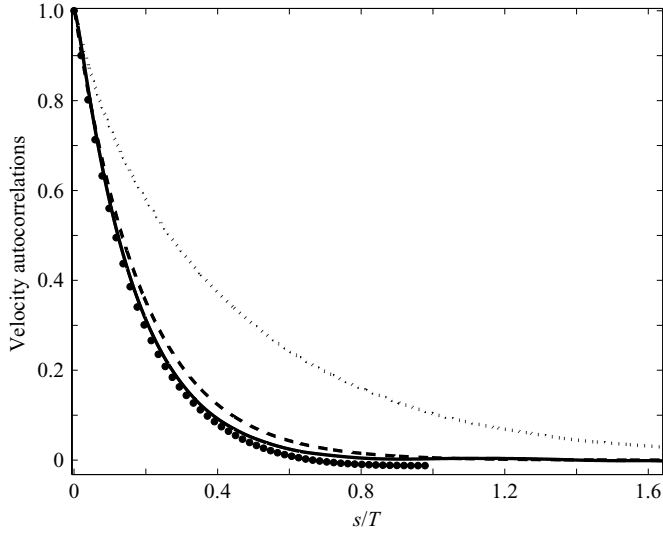
FIGURE 7. Velocity autocorrelations from CCG simulations based on (5.2)–(5.3) (solid), Sawford 1991 (dashed) and Reynolds 2003 (dotted) models compared to component-averaged data at $R_\lambda \approx 650$ from 2048^3 DNS (symbols).
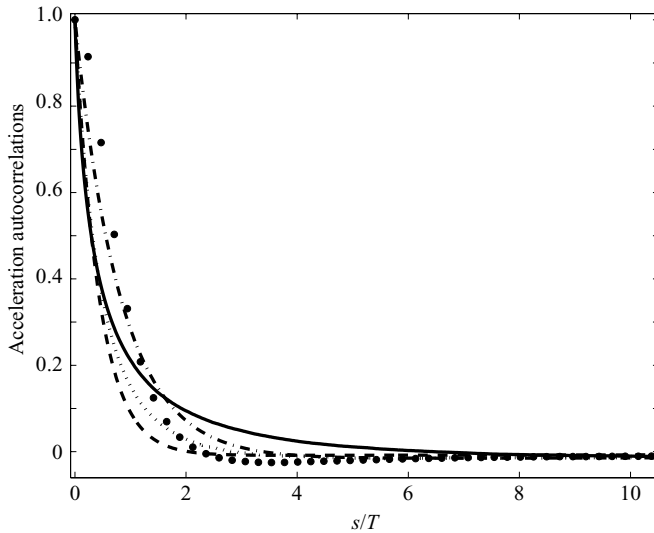

FIGURE 8. Acceleration autocorrelations from CCG simulations based on (5.2)–(5.3) (solid), Sawford 1991 (dashed), Sawford 1991 with a_0 from Sawford *et al.* (2003) (dot-dashed) and Reynolds 2003 (dotted) models compared to component-averaged data at $R_\lambda \approx 650$ from 2048^3 DNS (symbols).

the stochastic models yield a non-differentiable acceleration and, correspondingly, the acceleration autocorrelation has a negative slope at the origin. Since acceleration is the derivative of a stationary random process (i.e. $A(t) = \mathrm{d}U(t)/\mathrm{d}t$), the integral of its autocorrelation is zero. The CCG prediction in figure 8 does not clearly display the negative portion evident in the DNS data, and hence raises questions about the satisfaction of this integral property. However, closer examination reveals that the
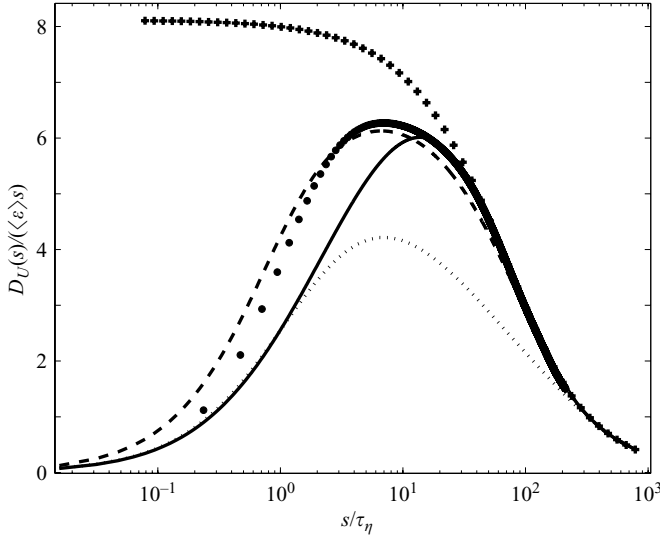
FIGURE 9. Second-order Lagrangian velocity structure functions from CCG simulations based on (5.2)–(5.3) (solid), Sawford 1991 (dashed), Reynolds 2003 (dotted) and velocity–dissipation (+ marks) models compared to data at $R_\lambda \approx 650$ from 2048^3 DNS (circles).

autocorrelation has a long negative region of very small amplitude, and that its integral is indeed zero. The agreement between the Sawford (1991) model and the DNS data is improved if the specification of $a_0 = 0.13R_\lambda^{0.64}$ is changed to $a_0 = 5/(1 + 110/R_\lambda)$, as suggested by Sawford *et al.* (2003).

The second-order Lagrangian velocity structure functions (divided by $\langle \varepsilon \rangle s$) are shown in figure 9. Except at small times ($s/\tau_\eta < 10$), the CCG model agrees well with the DNS data; but at small times there are discrepancies of around 30 %. (This is inevitable given the behaviour of the acceleration autocorrelations observed in figure 8.) At very small times, $D_U(s)$ equals $\langle A^2 \rangle s^2$ (to leading order) and hence the model again agrees with the DNS data (because, by construction, $\langle A^2 \rangle$ is modelled accurately). While the velocity–dissipation model shows good agreement at large times ($s/\tau_\eta \gtrsim 50$), at smaller times the prediction of $D_U(s)/(\langle \varepsilon \rangle s)$ tends to a constant, corresponding to the acceleration being modelled as white noise. The Sawford (1991) model is close to the DNS data.

6.2. *Conditional statistics*

Figure 10 shows the conditional Lagrangian velocity autocorrelations

$$\rho_{U|\varphi}(s|\hat{\varphi}) \equiv \langle U(s)U(0)|\varphi(0) = \hat{\varphi} \rangle / \langle U(0)^2 \rangle, \qquad (6.1)$$

given by the CCG model for five values of the conditioning variable $\hat{\varphi}$ compared to the DNS data. There is uniformly excellent agreement.

We define the velocity halving time $\tau_{U|\varphi}(\hat{\varphi})$ as the time interval for which $\rho_{U|\varphi}(s|\hat{\varphi})$ equals a half, i.e. such that

$$\rho_{U|\varphi}(\tau_{U|\varphi}(\hat{\varphi})|\hat{\varphi}) = \tfrac{1}{2}. \qquad (6.2)$$

This provides a characterization of the dependence of the velocity autocorrelation time scale on the pseudo-dissipation. In figure 11, this halving time is plotted against the value of the pseudo-dissipation used in the conditioning for the DNS and three stochastic models. In essence, the diffusion coefficient in the CCG model $\bar{b}(\hat{\varphi})$ is
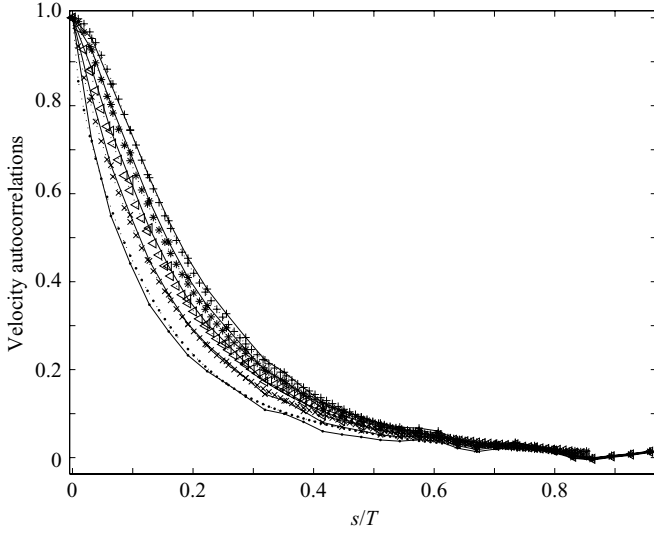
FIGURE 10. Conditional velocity autocorrelations for CCG model (solid) based on (5.2)–(5.3) compared to data at $R_\lambda \approx 650$ from 2048^3 DNS (dotted). The symbols {+, *, triangle, ×, small circle} correspond to the values {−2.05, −0.994, 0, 0.994, 2.05} of the conditioning variable $(\ln \varphi - \langle \ln \varphi \rangle)/\sigma_{\ln \varphi}$.
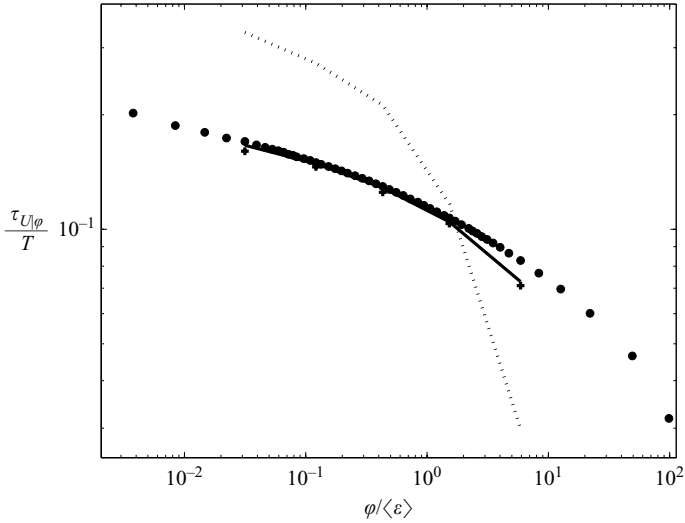

FIGURE 11. Model predictions for halving times of conditional velocity autocorrelations from CCG simulations based on (5.2)–(5.3) (solid) and Reynolds 2003 (dotted) and velocity–dissipation (+ marks) models compared to data at $R_\lambda \approx 650$ from 2048^3 DNS (circles).

chosen to match the conditional velocity statistics in this time range, and so the good agreement between the CCG model prediction and the DNS observed in figure 11 is not surprising. In contrast, for the Reynolds model, the diffusion coefficient is chosen by analogy with the Sawford (1991) model. This leads to a velocity conditional time scale that varies as $\mathcal{T}_{L,\varphi}(\hat{\varphi}) \sim (\hat{\varphi}/\langle \varepsilon \rangle)^{-1}$ for all $\hat{\varphi}$, at variance with the DNS data
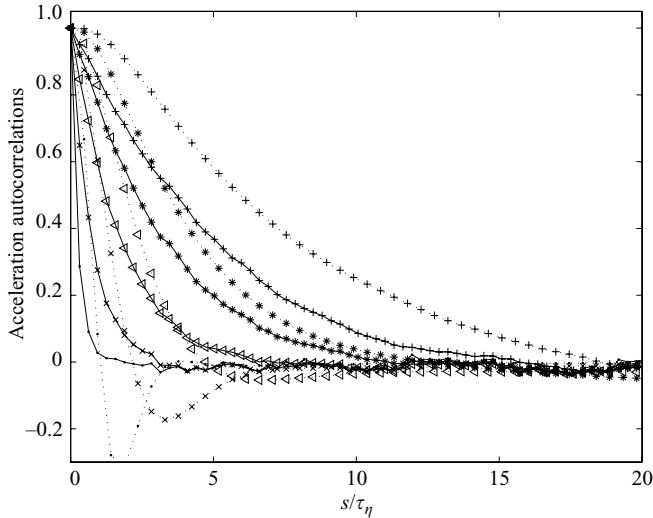
FIGURE 12. Conditional acceleration autocorrelations for CCG model (solid) based on (5.2)–(5.3) compared to data at $R_\lambda \approx 650$ from 2048^3 DNS (dotted). The symbols $\{+, *,$ triangle, $\times$, small circle$\}$ correspond to the values $\{-2.05, -0.994, 0, 0.994, 2.05\}$ of the conditioning variable $(\ln \varphi - \langle \ln \varphi \rangle)/\sigma_{\ln \varphi}$.

(equations (5.2)–(5.3)). As a result, $\tau_{U|\varphi}$ for the Reynolds model falls off faster with $\hat{\varphi}/\langle \varepsilon \rangle$ than for the other curves in figure 11.

Figure 12 shows the conditional acceleration autocorrelations given by the CCG model compared to the DNS. For the same reason as for the unconditional acceleration autocorrelation (figure 8), the agreement is poor.

Conditional second-order Lagrangian velocity structure functions $D_{U|\varphi}(s|\hat{\varphi})$ normalized by $\langle \varepsilon \rangle s$ have already been presented in figure 5. For all values of the pseudo-dissipation, there is good agreement between the CCG model and the DNS for times $s/\tau_\eta \gtrsim 20$. For the smallest values of φ, this good agreement extends to all times; but for the larger values of φ there are substantial discrepancies, with the CCG model significantly underpredicting the peak value of $D_{U|\varphi}(s|\hat{\varphi})/(\langle \varepsilon \rangle s)$. For very small times, $D_{U|\varphi}(s|\hat{\varphi})$ tends to $s^2 \sigma_{A|\varphi}^2$, and hence the model again agrees with the DNS data.

For $s/\tau_\eta \gtrsim 20$, the velocity–dissipation model yields accurate predictions of $D_{U|\varphi}$, but for smaller times the model predicts that $D_{U|\varphi}(s|\hat{\varphi})/(\langle \varepsilon \rangle s)$ tends to a constant $\hat{C}_0(\hat{\varphi})$, which increases with φ, specifically

$$\hat{C}_0(\hat{\varphi}) = \frac{4}{3}\left[\alpha + \beta \left(\frac{\hat{\varphi}}{\langle \varepsilon \rangle}\right)^{1/2}\right]. \tag{6.3}$$

6.3. *Variations with Reynolds number*

The results shown above pertain to a single Reynolds number, the highest attained in the DNS ($R_\lambda \approx 650$).

Figure 13 shows the variation with R_λ of the Lagrangian velocity integral time scale T_L (normalized by $T \equiv (3/2)\sigma_U^2/\langle \varepsilon \rangle$). The DNS clearly show that T_L/T decreases with R_λ. It should be appreciated that the observed values of T_L/T may not be universal, but may depend on the details of the forcing used in the DNS. In general, the CCG model is in good agreement with the DNS. The prediction of the velocity–dissipation
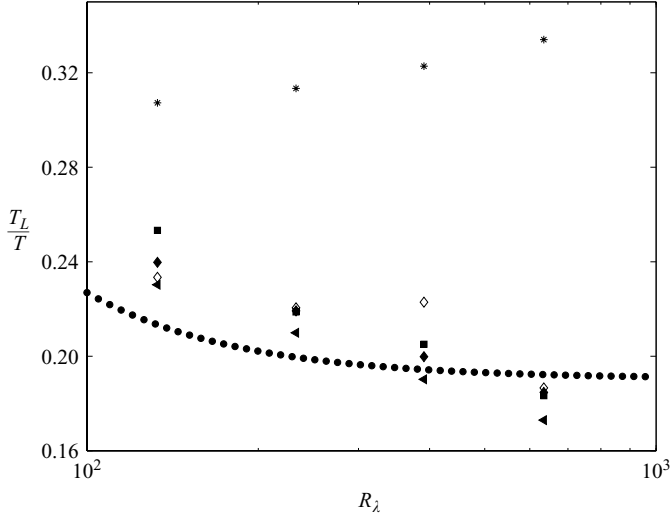
FIGURE 13. Model predictions for Lagrangian velocity integral time scales from CCG simulations based on (5.2) and figure 6 (open diamonds) and (5.2)–(5.3) (closed diamonds) and velocity-dissipation (triangles) and Reynolds 2003 (stars) and Sawford 1991 (circles) models compared to DNS data (squares).

model is similar, but some 5% below that of the CCG model. The Sawford model predicts comparable values of T_L/T and a weaker decrease with R_λ than indicated by the DNS data. In contrast, the values given by the Reynolds model are up to 50% larger and increase with R_λ.

The Reynolds-number dependence of the peak of the normalized structure function $D_U(s)/(\langle\varepsilon\rangle s)$, denoted by $\mathscr{C}_0^*$ (first studied by Yeung & Pope 1989), is of special significance since according to the Kolmogorov (1941) hypotheses it is expected to approach the Lagrangian Kolmogorov constant $\mathscr{C}_0$ for an inertial range $\tau_\eta \ll s \ll T_L$ at high Reynolds number. The inference of an asymptotic value of $\mathscr{C}_0$ from $\mathscr{C}_0^*$ at moderate Reynolds numbers (e.g. Sawford 1991; Sawford & Yeung 2001) is an important modelling issue where projections from available DNS data may be helpful (Sawford & Yeung 2001 and Yeung 2002 provide estimates in the range 6–7). The variation of $\mathscr{C}_0^*$ with R_λ is shown in figure 14 for the DNS and for four stochastic models. As may be seen, the values of $\mathscr{C}_0^*$ obtained from DNS increase with R_λ, as they do for all of the models. The CCG and Sawford models yield similar predictions with comparable agreement with the DNS data over the range of R_λ examined. In contrast, the values of $\mathscr{C}_0^*$ given by the Reynolds model are up to 22% lower than the DNS and those of the velocity–dissipation model are up to 35% higher.

As the Reynolds number tends to infinity, the Sawford model predicts that $\mathscr{C}_0^*$ tends to a constant, specifically $\mathscr{C}_0$. For the velocity–dissipation model we have

$$\mathscr{C}_0^* = \frac{4}{3}\left\langle \frac{T}{\mathscr{T}_{L,\varphi}} \right\rangle$$
$$= \frac{4}{3}\left(\alpha + \beta\left\langle \left(\frac{\varphi}{\langle\varepsilon\rangle}\right)^{1/2}\right\rangle\right)$$
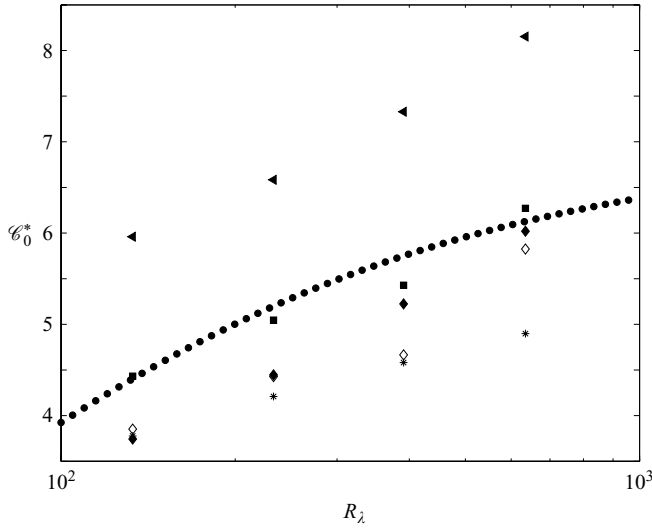$$\approx 3.87 + 0.237 R_\lambda^{0.453}, \qquad (6.4)$$

FIGURE 14. Model predictions for $\mathscr{C}_0^*$ from CCG simulations based on (5.2) and figure 6 (open diamonds) and (5.2)–(5.3) (closed diamonds) and velocity–dissipation (triangles) and Reynolds 2003 (stars) and Sawford 1991 (circles) models compared to DNS data (squares).

where in the final step we have used $\langle(\varphi/\langle\varepsilon\rangle)^{1/2}\rangle = \exp(-\sigma_\chi^2/8)$ and (2.2) for σ_χ^2. Thus, the velocity–dissipation model predicts an increase of $\mathscr{C}_0^*$ as $R_\lambda^{0.453}$, and presumably so also does the CCG model. While the experimental data of Ouellette *et al.* (2006) suggest that $\mathscr{C}_0^*$ achieves an asymptote, this is, as yet, far from certain.

7. Conclusions

After a brief review of the basis for the Reynolds (2003) model against DNS, we have shown the formulation of a novel stochastic model based on simple data parameterizations from DNS. The model consists of three stochastic differential equations ((3.2), (3.3) and (3.4)) with the coefficients σ_χ^2, T_χ, $\sigma_{A|\varphi}$ and $\bar{b}^2$ given by (2.2), (2.3), (2.6), (5.1)–(5.3), and with $p = 0.1$. This model is exactly consistent with Gaussian velocity and conditionally cubic-Gaussian acceleration statistics and incorporates a representation for the logarithm of pseudo-dissipation as an Ornstein–Uhlenbeck process. The new model captures the effects of intermittency of dissipation on acceleration and the deviations from the Kolmogorov (1962) hypotheses (based on the DNS reported in (Yeung *et al.* 2007) in the conditional dependence of acceleration on pseudo-dissipation. Further, non-Gaussianity of the conditionally standardized acceleration PDF (as observed in DNS) is captured in terms of model nonlinearity. Thus, by construction, the model provides an accurate description of the one-time joint PDF of velocity, acceleration and pseudo-dissipation, and this one-time PDF is unaffected by the specified diffusion coefficient $\bar{b}$. This coefficient is specified by attempting to match the two-time conditional velocity statistics, which is successful for low pseudo-dissipation, and for not too small times, $s/\tau_\eta > 20$. The unconditional and conditional velocity autocorrelations are in excellent agreement with the DNS data (figures 7 and 10). The acceleration autocorrelations (figures 8 and 12) given by the model differ from those observed in DNS, which is probably inevitable for a model of this form. This shortcoming could probably be overcome in a higher-order model (in which one or more derivatives of acceleration are represented), but at the cost of

added complexity and difficulty in determining the appropriate model coefficients. The model does not account for the conditional dependence of acceleration on velocity, as observed in DNS and experiments (Sawford *et al.* 2003).

The corresponding velocity–dissipation model provides no realistic representation for acceleration or small-time statistics, but it accurately represents the conditional and unconditional velocity statistics on time scales large compared to the Kolmogorov time scale (figures 7 and 10). In computer simulations, the velocity–dissipation model is much less expensive than the CCG model, because its time-step requirement ($\Delta t / T_\chi \ll 1$) is much less restrictive than that of the CCG model (which is $\Delta t / \tau_\eta \ll 1$). The form of the velocity–dissipation model is the same as that proposed by Pope & Chen (1990), but the form of the conditional time scale $\mathcal{T}_{L,\varphi}$ is rather different. In contrast to (5.2), in the Pope & Chen (1990) model, $T / \mathcal{T}_{L,\varphi}$ varies directly as $\varphi / \langle \varepsilon \rangle$. The Pope & Chen (1990) model is independent of Reynolds number, whereas the present velocity–dissipation model contains Reynolds-number-dependent parameters. Such Reynolds-number dependence is clearly necessary for the model to reproduce the conditional statistics in the inertial range which display a clear Reynolds-number dependence (see, e.g. figure 6).

Inertial-range non-Gaussian statistics of the Lagrangian velocity increments and the long-time correlation of the magnitude of acceleration have been reported in experiments (e.g. Mordant *et al.* 2002, 2003) and numerical simulations (Bec *et al.* 2006). A detailed analysis of the model's performance in these respects is left for future investigations.

In summary, the main advantage offered by the CCG model is that it allows access to conditional statistics of velocity and acceleration. This permits an accurate representation (at the one-time level) of the DNS data on the Lagrangian acceleration PDF and (at the two-time level) of the DNS data on conditional and unconditional velocity autocorrelations and time scales.

Appendix A. Derivation of the corresponding velocity–dissipation model

The CCG model is a coupled set of three stochastic differential equations for $U(t)$, $A(t)$ and $\chi(t)$ (equations (3.2)–(3.4)). In this Appendix, we use adiabatic elimination to deduce the corresponding velocity–dissipation model, consisting of a pair of SDEs for $U(t)$ and $\chi(t)$ (equations (4.6)–(4.7)). The velocity–dissipation model generates statistics which approximate those of the CCG model.

The CCG model is a dynamical system defined by stochastic equations characterized by time scales T, τ_η and T_χ (which is of the same order as T). The time scale $T \equiv 1.5\sigma_U^2 / \langle \varepsilon \rangle$ characterizes the velocity $U(t)$, whereas the Kolmogorov temporal microscale $\tau_\eta \equiv \sqrt{\nu / \langle \varepsilon \rangle}$ is appropriate for describing the evolution of $A(t)$. At high Reynolds number, T is widely separated from τ_η and A is a 'fast' variable compared to U. It will be shown that, in the limit as the Reynolds number grows unbounded, $U(t)$ evolves by the SDE which involves the conditional time scale $\mathcal{T}_{L,\varphi}$. In the following, a simplified analysis is performed to determine this velocity conditional time scale $\mathcal{T}_{L,\varphi}(\chi)$.

The analysis is based on the Fokker–Planck equation obtained from (3.2)–(3.4) which describes the evolution of the joint PDF of $U(t)$, $\bar{A}(t)$ and $\chi^*(t)$. The normalized dependent variables considered are $U(t)/\sigma_U$, $\bar{A}(t)$ and $\chi^*(t)/\sigma_\chi$, and $\bar{v}$, $\bar{a}$ and $\bar{x}$ are introduced as corresponding sample-space variables. The normalized independent variable used is

$$\tau = \frac{a_\eta}{\sigma_U} t, \tag{A 1}$$

and we define the small parameter ξ by

$$\xi \equiv \frac{u_\eta}{\sigma_U} = \frac{15^{1/4}}{\sqrt{R_\lambda}}, \tag{A 2}$$

where u_η, the Kolmogorov velocity scale, is defined by $u_\eta \equiv (\nu\langle\varepsilon\rangle)^{1/4}$. It then follows that the one-time joint PDF of $\{U(t)/\sigma_U, \bar{A}(t), \chi^*(t)/\sigma_\chi\}$, denoted by $f(\bar{v}, \bar{a}, \bar{x}; \tau)$, evolves by the Fokker–Planck equation

$$\xi \left\{ \frac{\partial}{\partial \tau} + \underbrace{\frac{\sigma_{A|\varphi}}{a_\eta}}_{S} \left[(c_1\bar{a} + c_2\bar{a}^3)\frac{\partial}{\partial\bar{v}} - 2c_2\bar{v}\bar{a} - \bar{v}(c_3 + c_2\bar{a}^2)\frac{\partial}{\partial\bar{a}} \right] \right\} f$$

$$= \underbrace{\frac{\tau_\eta\bar{b}^2}{2}}_{\mathscr{B}} \mathscr{L}_{\bar{a}}f + \tfrac{2}{3}\xi^2 h \mathscr{L}_{\bar{x}}f, \tag{A 3}$$

where $S \equiv \sigma_{A|\varphi}/a_\eta$, $\mathscr{B} \equiv \frac{1}{2}\tau_\eta\bar{b}^2$, $h \equiv T/T_\chi$, $\mathscr{L}_y \equiv \partial/\partial y(y + \partial/\partial y)$, and $c_1 = C(1-p) \approx 0.73$, $c_2 = Cp \approx 0.081$ and $c_3 = C(1+p) \approx 0.89$.

In (A 3), the small parameter ξ appears directly (as ξ and ξ^2 in the first and last terms), and also indirectly through the Reynolds-number dependence of several coefficients. In the analysis, we consider a high Reynolds number, we take the coefficients S, $\mathscr{B}$ and h to be fixed (based on the Reynolds number), and then consider the limit as ξ tends to zero. Thus, with the coefficients $S(\bar{x})$, $\mathscr{B}(\bar{x})$ and h being considered fixed, (A 3) can be rewritten in the form

$$\xi \left\{ \frac{\partial}{\partial \tau} + \mathscr{S} \right\} f = \mathscr{B}\mathscr{L}_{\bar{a}}f + \tfrac{2}{3}\xi^2 h \mathscr{L}_{\bar{x}}f, \tag{A 4}$$

where $\mathscr{S} \equiv S[(c_1\bar{a} + c_2\bar{a}^3)(\partial/\partial\bar{v}) - 2c_2\bar{v}\bar{a} - \bar{v}(c_3 + c_2\bar{a}^2)\partial/\partial\bar{a}]$.

The analysis is complicated because a regular perturbative treatment of (A 4) fails in the large-time limit, i.e.

$$f = f^{(0)} + \xi f^{(1)} + \xi^2 f^{(2)} + \cdots, \tag{A 5}$$

is not uniformly convergent for small ξ. However, a successful analysis can be performed using the method of multiple scales. The joint PDF in (A 4) is treated as a function of several time scales

$$\tau_0 = \tau, \quad \tau_1 = \xi\tau, \quad \tau_2 = \xi^2\tau, \cdots, \tag{A 6}$$

so that

$$\frac{\partial}{\partial\tau} \rightarrow \frac{\partial}{\partial\tau_0} + \xi\frac{\partial}{\partial\tau_1} + \xi^2\frac{\partial}{\partial\tau_2} + \cdots. \tag{A 7}$$

The joint PDF f is considered to depend on all of these time scales, and it is then expanded in powers of ξ as in (A 5). The solution is eventually obtained by restricting

the auxiliary time variables to the line (A 6). The fact that $f(\bar{v}, \bar{a}, \bar{x}; \tau_0, \tau_1, \tau_2, \cdots)$ has no physical meaning outside the line (A 6) is exploited to enforce conditions that prevent loss of asymptoticness of (A 5) for $\tau \geqslant O(\xi^{-1})$ in the regular perturbation.

Substituting (A 5) into the governing equation (A 4) and comparing coefficients of equal powers of ξ yields a sequence of problems. At $O(1)$ (A 4) is

$$\mathscr{L}_{\bar{a}} f^{(0)} = 0, \tag{A 8}$$

whence

$$f^{(0)}(\bar{v}, \bar{a}, \bar{x}; \tau_0, \tau_1, \tau_2, \cdots) = \Phi(\bar{v}, \bar{x}; \tau_0, \tau_1, \tau_2, \cdots)\frac{\exp(-\bar{a}^2/2)}{\sqrt{2\pi}}, \tag{A 9}$$

where Φ (with the time scales restricted to (A 6)) is the joint PDF of $(U/\sigma_U, \chi^*/\sigma_\chi)$ at leading order. At $O(\xi)$, (A 4) is

$$\mathscr{B}\mathscr{L}_{\bar{a}} f^{(1)} = \left\{ \frac{\partial}{\partial \tau_0} + \mathscr{S} \right\} f^{(0)}. \tag{A 10}$$

The solvability condition at $O(\xi)$ is $\partial \Phi / \partial \tau_0 = 0$ and we then find

$$f^{(1)}(\bar{v}, \bar{a}, \bar{x}; \tau_0, \tau_1, \tau_2, \cdots) = -\left(c_3 \bar{a} + \frac{c_2}{3}\bar{a}^3 \right) \frac{S}{\mathscr{B}} \frac{e^{-\bar{a}^2/2}}{\sqrt{2\pi}} \left[\frac{\partial \Phi}{\partial \bar{v}} + \bar{v}\Phi \right]$$

$$+ \Psi(\bar{v}, \bar{x}; \tau_0, \tau_1, \tau_2, \cdots)\frac{\exp(-\bar{a}^2/2)}{\sqrt{2\pi}}, \tag{A 11}$$

where Ψ (with the time scales restricted to (A 6)) is the joint PDF of $(U/\sigma_U, \chi^*/\sigma_\chi)$ at first order. At $O(\xi^2)$, (A 4) is

$$\mathscr{B}\mathscr{L}_{\bar{a}} f^{(2)} = \left\{ \frac{\partial}{\partial \tau_0} + \mathscr{S} \right\} f^{(1)} + \frac{\partial}{\partial \tau_1} f^{(0)} - \tfrac{2}{3}h\mathscr{L}_{\bar{x}} f^{(0)}, \tag{A 12}$$

which implies the following solvability condition

$$\frac{\partial \Phi}{\partial \tau_1} = \frac{\delta S^2}{\mathscr{B}} \mathscr{L}_{\bar{v}}\Phi + \tfrac{2}{3}h\mathscr{L}_{\bar{x}}\Phi, \tag{A 13}$$

where $\delta \equiv c_1^2 + 6c_1 c_2 + 11c_2^2$.

We use these results to obtain an evolution equation for the joint PDF of velocity and dissipation. In terms of the non-dimensional variables $(U/\sigma_U, \chi^*/\sigma_\chi)$, this joint PDF is denoted by $\bar{F}(\bar{v}, \bar{x}; \tau)$, and can be obtained from $f(\bar{v}, \bar{a}, \bar{x}; \tau)$ by integrating over $\bar{a}$. The equivalent joint PDF of the dimensional variables is denoted by $F(v, x^*; t)$. The solvability conditions above are employed to simplify $\partial \bar{F}/\partial \tau$, which leads to the following governing equation:

$$\frac{\partial \bar{F}}{\partial \tau} = \xi \left[\frac{\delta S^2}{\mathscr{B}} \mathscr{L}_{\bar{v}}\bar{F} + \tfrac{2}{3}h\mathscr{L}_{\bar{x}}\bar{F} \right] + O(\xi^2). \tag{A 14}$$

In terms of dimensional variables (and to leading order in ξ), (A 14) can be recast in the form

$$\frac{\partial F}{\partial t} = \frac{3\delta S^2}{2\mathscr{B}} \left[\frac{\partial}{\partial v}\left(\frac{v}{T}F \right) + \frac{\sigma_U^2}{T} \frac{\partial^2 F}{\partial v^2} \right] + \frac{\partial}{\partial x^*}\left(\frac{x^*}{T_\chi}F \right) + \frac{\sigma_\chi^2}{T_\chi} \frac{\partial^2 F}{\partial x^{*2}}. \tag{A 15}$$

This is the Fokker–Planck equation corresponding to the velocity–dissipation model (4.6), (4.7) with

$$\frac{\mathscr{T}_{L,\varphi}}{T} = \frac{2\mathscr{B}}{3\delta S^2}. \tag{A 16}$$

Given the relation $\tau_\eta \bar{b}^2 = 2\mathscr{B}$, it can be seen that there is a one-to-one correspondence between the diffusion coefficient in the CCG model and the conditional time scale in the velocity–dissipation model, i.e.

$$\bar{b}^2 = \frac{3\delta S^2}{\tau_\eta} \frac{\mathscr{T}_{L,\varphi}}{T}. \qquad (A\,17)$$

When used in conjunction with (5.2), the result of this analysis is not consistent with the premise of frozen ξ-dependences for the coefficients. Specifically, for large $\bar{x}$, $\mathscr{B}$ varies as $\xi \ln(1/\xi^2)$. Nevertheless, the numerical tests in figure 4 show that the adiabatic elimination result (A 16) is (in some sense) accurate.

Appendix B. Velocity autocorrelations in velocity–dissipation model

Following the approach of Pope & Chen (1990), in this Appendix we derive exact and approximate relations for the velocity autocorrelations implied by the velocity–dissipation model:

$$dU = -\frac{U}{\mathscr{T}_{L,\varphi}}\,dt + \sqrt{\frac{2\sigma_U^2}{\mathscr{T}_{L,\varphi}}}\,dW, \qquad (B\,1)$$

$$d\chi^* = -\chi^* \frac{dt}{T_\chi} + \sqrt{\frac{2\sigma_\chi^2}{T_\chi}}\,dW'. \qquad (B\,2)$$

Since the χ^* equation is effectively decoupled from the U equation, the velocity is governed by a linear SDE with random drift and diffusion coefficients. Without loss of generality, the evolution of $\chi(t)$ subject to the condition $\{\chi(0) = \hat{\chi}\}$ is considered.

We define a stochastically scaled time by

$$r(t|\hat{\chi}) \equiv \int_0^t \frac{\mathscr{T}_{L,\varphi}(\hat{\chi})}{\mathscr{T}_{L,\varphi}(\chi(t';\hat{\chi}))}\,dt', \qquad (B\,3)$$

where $\chi(t;\hat{\chi})$ denotes an Ornstein–Uhlenbeck process started at $\chi(0) = \hat{\chi}$. Further, Levy's theorem (e.g. Protter 2004) can be invoked to show that

$$\widetilde{W}(r|\hat{\chi}) = \int_0^t \sqrt{\frac{\mathscr{T}_{L,\varphi}(\hat{\chi})}{\mathscr{T}_{L,\varphi}(\chi(t';\hat{\chi}))}}\,dW(t') \qquad (B\,4)$$

is a standard Brownian motion in stochastically scaled time r. Then, it is easily seen that (B 1) defines an Ornstein–Uhlenbeck process in stochastically scaled time, $\tilde{U}(r) = U(t|\hat{\chi})$, i.e.

$$d\tilde{U}(r) = -\frac{\tilde{U}(r)}{\mathscr{T}_{L,\varphi}(\hat{\chi})}\,dr + \sqrt{\frac{2\sigma_U^2}{\mathscr{T}_{L,\varphi}(\hat{\chi})}}\,d\widetilde{W}(r). \qquad (B\,5)$$

The $\tilde{U}(r)$ process has zero mean and autocorrelation given by

$$\tilde{\rho}(t|\hat{\chi}) = \left\langle \exp\left(-\frac{r(t|\hat{\chi})}{\mathscr{T}_{L,\varphi}(\hat{\chi})}\right) \right\rangle_{W'}, \qquad (B\,6)$$

where $\langle \cdots \rangle_{W'}$ denotes averaging over the realizations of the $\chi(t;\hat{\chi})$ process. As a result, the velocity autocorrelation conditional on $\{\chi(0) = \hat{\chi}\}$ can be written in the

form

$$\rho_U(t|\hat{\chi}) = \left\langle \exp\left(-\int_0^t \frac{\mathrm{d}t'}{\mathscr{T}_{L,\varphi}(\chi(t';\hat{\chi}))}\right)\right\rangle_{W'}. \tag{B 7}$$

This expression is developed further for the specification of $\mathscr{T}_{L,\varphi}$ used in the model. This is (5.2), which can be rewritten as

$$\frac{T}{\mathscr{T}_{L,\varphi}} = \alpha + \beta \exp(\gamma\chi(t)). \tag{B 8}$$

An approximate expression for the unconditional autocorrelation ρ_U will be obtained that involves the integral scale of $\Gamma(t) \equiv (\varphi(t)/\langle\varepsilon\rangle)^\gamma = e^{\gamma\chi(t)}$. Now, since $\chi(t)$ is a stationary Gaussian process with autocorrelation $\rho_\chi(s) = \exp(-|s|/T_\chi)$, the autocorrelation of Γ is given by:

$$\rho_\Gamma(s) = \frac{\exp\left(\gamma^2\sigma_\chi^2 e^{-|s|/T_\chi}\right) - 1}{\exp\left(\gamma^2\sigma_\chi^2\right) - 1}. \tag{B 9}$$

Hence, the integral scale of Γ can be written as

$$\frac{T_\Gamma}{T_\chi} = \int_0^\infty \rho_\Gamma(s)\,\mathrm{d}s = \frac{1}{\exp\left(\gamma^2\sigma_\chi^2\right) - 1}\left[\mathrm{Ei}\left(\gamma^2\sigma_\chi^2\right) - \ln\left(\gamma^2\sigma_\chi^2\right) - \bar{\gamma}\right], \tag{B 10}$$

where Ei is the exponential integral and $\bar{\gamma}$ is Euler's constant. Substituting (5.2) into (B 7) and averaging over the initial (random) dissipation yields the unconditional velocity autocorrelation

$$\rho_U(t) = \exp\left(-\alpha\frac{t}{T}\right)\left\langle\exp\left(-\beta\frac{\bar{r}(t)}{T}\right)\right\rangle, \tag{B 11}$$

where the stochastically scaled time is in this case $\bar{r}(t) \equiv \int_0^t \Gamma(t')\,\mathrm{d}t'$. An approximate expression for the right-hand side of (B 11) can be obtained by introducing a log-normal assumption for the one-time distribution of $\bar{r}(t)$. The mean and variance of $\bar{r}(t)$ are easily computed as $\langle\bar{r}(t)\rangle = C_\gamma t$ (with $C_\gamma \equiv \exp(\gamma(\gamma-1)\sigma_\chi^2/2)$) and

$$\mathrm{var}(\bar{r}(t)) = 2\Gamma'^2\int_0^t (t-s)\rho_\Gamma(s)\,\mathrm{d}s, \tag{B 12}$$

where $\Gamma'^2 \equiv C_\gamma^2(\exp(\gamma^2\sigma_\chi^2) - 1)$. To perform the integral on the right-hand side analytically, an exponential approximation $\rho_\Gamma(s) \approx \exp(-s/T_\Gamma)$ to the autocorrelation (B 9) is employed. Equation (B 12) then becomes

$$\mathrm{var}(\bar{r}(t)) \approx 2\Gamma'^2 T_\Gamma^2\left[\exp(-t/T_\Gamma) + \frac{t}{T_\Gamma} - 1\right]. \tag{B 13}$$

Assuming that $\bar{r}(t)$ is log-normal, i.e. $\bar{r}(t)/\langle r(t)\rangle = \exp(q(t))$, where $q(t) \sim \mathcal{N}(-\Sigma(t)^2/2, \Sigma(t)^2)$ with

$$\Sigma(t)^2 = \ln\left(\frac{\langle\bar{r}(t)^2\rangle}{C_\gamma^2 t^2}\right) = \ln\left\{1 + 2\Gamma'^2\frac{T_\Gamma^2}{C_\gamma^2 t^2}\left[\exp(-t/T_\Gamma) + \frac{t}{T_\Gamma} - 1\right]\right\}, \tag{B 14}$$

we find

$$\rho_U(t) \approx \exp\left(-\alpha\frac{t}{T}\right)\left\langle\exp\left(-e^{q(t)}\frac{\beta C_\gamma t}{T}\right)\right\rangle = \frac{\exp\left(-\alpha\frac{t}{T}\right)}{\sqrt{2\pi}}$$
$$\times \int_{-\infty}^\infty \exp\left\{-\frac{\beta C_\gamma t}{T}\exp\left(\Sigma(t)\left(y - \frac{\Sigma(t)}{2}\right)\right) - \frac{y^2}{2}\right\}\mathrm{d}y. \tag{B 15}$$
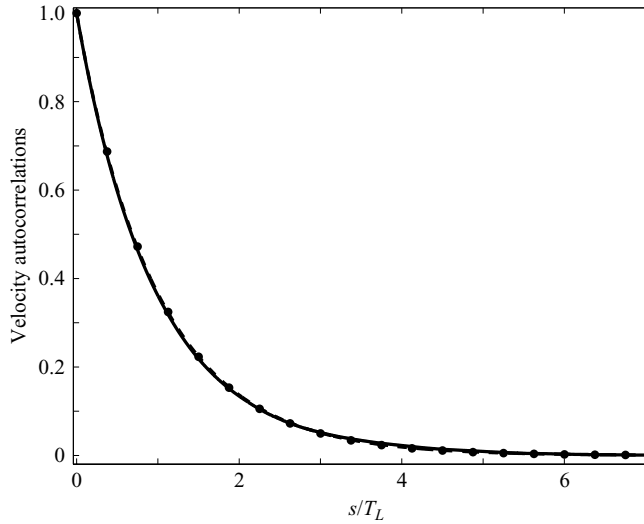
FIGURE 15. Velocity autocorrelations from simulations of the velocity–dissipation model at $R_\lambda = 650$ (solid) compared to approximate autocorrelation (B 15) (dashed) and exponential approximation (circles).

In figure 15, the approximate expression (B 15) is compared to the autocorrelation obtained from SDE simulation of the velocity–dissipation model and to a simple exponential. The maximum absolute errors between the SDE simulation and the other two curves are less than 3%. Therefore, the approximations on which (B 15) is based (i.e. that Γ has an exponential autocorrelation and that $\bar{r}$ is log-normally distributed) do not invalidate its accuracy.

In summary, the principal results obtained in this Appendix are an exact formula, (B 7), for the conditional velocity autocorrelation of the velocity–dissipation model and an approximate expression, (B 15), for its unconditional velocity autocorrelation.

REFERENCES

BEC, J., BIFERALE, L., CENCINI, M., LANOTTE, A. & TOSCHI, F. 2006 Effects of vortex filaments on the velocity of tracers and heavy particles in turbulence. *Phys. Fluids* **18**, 081702.

BECK, C. 2002 Lagrangian acceleration statistics in turbulent flows. *Europhys. Lett.* **64**, 151–157.

BIFERALE, L., BOFFETTA, G., CELANI, A., LANOTTE, A. & TOSCHI, F. 2005 Particle trapping in three-dimensional fully developed turbulence. *Phys. Fluids* **17**, 021701.

CHRISTENSEN, K. T. & ADRIAN, R. J. 2002 Measurement of instantaneous Eulerian acceleration fields by particle image accelerometry: method and accuracy. *Exps. Fluids* **33**, 759–769.

FRISCH, U. 1995 *Turbulence*. Cambridge University Press.

GARDINER, C. W. 2004 *Handbook of Stochastic Methods*, 3rd edn. Springer.

GYLFASON, A., AYYALASOMAYAJULA, S. & WARHAFT, Z. 2004 Intermittency, pressure and acceleration statistics from hot-wire measurements in wind-tunnel turbulence. *J. Fluid Mech.* **501**, 213–229.

KOLMOGOROV, A. N. 1941 *Dokl. Akad. Nauk USSR* **30**, 299.

KOLMOGOROV, A. N. 1962 A refinement of previous hypotheses concerning the local structure of turbulence in a viscous compressible fluid at high Reynolds number. *J. Fluid Mech.* **13**, 82–85.

LA PORTA, A., VOTH, G. A., CRAWFORD, A. M., ALEXANDER, J. & BODENSCHATZ, E. 2001 Fluid particle accelerations in fully developed turbulence. *Nature* **409**, 1017–1019.

MORDANT, N., DELOUR, J., LÉVEQUE, E., ARNÉODO, A. & PINTON, J.-F. 2002 Long-time correlations in Lagrangian dynamics: a key to intermittency in turbulence. *Phys. Rev. Lett.* **89**, 254502.

Mordant, N., Delour, J., Léveque, E., Michel, O., Arnéodo, A. & Pinton, J.-F. 2003 Lagrangian velocity fluctuations in fully developed turbulence: scaling, intermittency, and dynamics. *J. Stat. Phys.* **113**, 701–717.

Mordant, N., Léveque, E. & Pinton, J.-F. 2004 Experimental and numerical study of the Lagrangian dynamics of high Reynolds number turbulence. *New J. Phys.* **6**, 116–159.

Ouellette, N. T., Xu, H., Bourgoin, M. & Bodenschatz, E. 2006 Small-scale anisotropy in Lagrangian turbulence. *New J. Phys.* **8**, 102.

Pope, S. B. 2002 A stochastic Lagrangian model for acceleration in turbulent flows. *Phys. Fluids* **14**, 2360–2375.

Pope, S. B. & Chen, Y. L. 1990 The velocity-dissipation probability density function model for turbulent flows. *Phys. Fluids* A **2**, 1437–1449.

Protter, P. E. 2004 *Stochastic Integration and Differential Equations*, 2nd edn. Springer.

Reynolds, A. M. 2003 Superstatistical mechanics of tracer-particle motions in turbulence. *Phys. Rev. Lett.* **91**, 084503.

Sawford, B. L. 1991 Reynolds number effects in Lagrangian stochastic models of turbulent dispersion. *Phys. Fluids* A **3**, 1577–1586.

Sawford, B. L. & Yeung, P. K. 2001 Langrangian statistics in uniform shear flow: direct numerical simulation and Lagrangian stochastic models. *Phys. Fluids* **13**, 2627–2634.

Sawford, B. L., Yeung, P. K., Borgas, M. S., Vedula, P., La Porta, A., Crawford, A. M. & Bodenschatz, E. 2003 Conditional and unconditional acceleration statistics in turbulence. *Phys. Fluids* **15**, 3478–3489.

Sreenivasan, K. R. & Kailasnath, P. 1993 Update on the intermittency exponent in turbulence. *Phys. Fluids* A **5**, 512–514.

Theiss, W. & Titulaer, U. M. 1985 The systematic adiabatic elimination of fast variables from a many dimensional Fokker–Planck equation. *Physica* A **130**, 123–142.

Vedula, P. & Yeung, P. K. 1999 Similarity scaling of acceleration and pressure statistics in numerical simulations of isotropic turbulence. *Phys. Fluids* **11**, 1208–1220.

Voth, G. A., Satyanarayan, K. & Bodenschatz, E. 1998 Lagrangian acceleration measurements at large Reynolds numbers. *Phys. Fluids* **10**, 2268–2280.

Voth, G. A., La Porta, A., Crawford, A. M., Alexander, J. & Bodenschatz, E. 2002 Measurement of particle accelerations in fully developed turbulence. *J. Fluid Mech.* **469**, 121–160.

Yeung, P. K. 1997 One- and two-particle Lagrangian acceleration correlations in numerically simulated homogeneous turbulence. *Phys. Fluids* **9**, 2981–2990.

Yeung, P. K. 2002 Lagrangian investigations of turbulence. *Annu. Rev. Fluid Mech.* **34**, 115–142.

Yeung, P. K. & Pope, S. B. 1989 Lagrangian statistics from direct numerical simulations of isotropic turbulence. *J. Fluid Mech.* **207**, 531–586.

Yeung, P. K., Pope, S. B., Lamorgese, A. G. & Donzis, D. A. 2006a Acceleration and dissipation statistics in numerically simulated isotropic turbulence. *Phys. Fluids* **18**, 065103.

Yeung, P. K., Pope, S. B. & Sawford, B. L. 2006b Reynolds number dependence of Lagrangian statistics in large numerical simulations of isotropic turbulence. *J. Turbulence* **7**, 1–12.

Yeung, P. K., Pope, S. B., Kurth, E. A. & Lamorgese, A. G. 2007 Lagrangian conditional statistics, acceleration and local relative motion in numerically simulated isotropic turbulence. *J. Fluid Mech.* **582**, 399–422.